Journal of Water Resource and Protection, 2025, 17(11), 727-747
https://www.scirp.org/journal/jwarp
ISSN Online: 1945-3108
ISSN Print: 1945-3094

Land Use and Land Cover Dynamics and Their Impact on the Water Body Regime in the Dallol Bosso Sub-Basin (West of Niger)

Bako Mamane[1,2], Sandao Issoufou[1,3*], Abdel Kader Hassane Saley[1], Mansour Mahamane[2]

[1]Faculty of Science, Technology, Department of Geology, University Abdou Moumouni, Niamey, Niger
[2]Department of Natural Resource Management, AGRHYMET Regional Center, Niamey, Niger
[3]Ministry of Environment, Water and Sanitation, Niamey, Niger
Email: *sandaoissoufou@gmail.com, mamane.bako@cilss.int, sandaoissoufou@gmail.com

How to cite this paper: Mamane, B., Issoufou, S., Saley, A.K.H. and Mahamane, M. (2025) Land Use and Land Cover Dynamics and Their Impact on the Water Body Regime in the Dallol Bosso Sub-Basin (West of Niger). *Journal of Water Resource and Protection*, **17**, 727-747.
https://doi.org/10.4236/jwarp.2025.1711039

Received: September 29, 2025
Accepted: November 2, 2025
Published: November 5, 2025

Abstract

In Niger, land use and land cover changes have affected hydrological processes and water regimes at various scales. However, the significant changes observed in land use and land cover dynamics over the past few decades have negatively impacted the living conditions of the population and the state of natural ecosystems, particularly in the Dallol Bosso sub-basin, where agriculture and livestock are the primary sources of income for the population. This paper investigates the dynamics and trends of changes in land use types and their relationships with surface water regimes over the last fifty years (1972-2023) in the Dallol Bosso sub-basin. To achieve this, the study employed data obtained from Landsat and Sentinel 2 during the years 1972, 1990, and 2023 and ground observation (water bodies' location and regime). Method and various geospatial analysis tools are used to estimate land use and land cover changes, monitoring land degradation. The result showed that the development of cultivation and settlement led to runoff (water erosion) and the emergence of ephemeral water bodies. The analysis of land use and land cover change indicates that settlement increased from 0.21% in 1972 to 0.5% in 2023 and that tiger bush and shrub savanna have declined considerably, by 1,332 hectares per year for tiger bush and 4,634 hectares per year for shrub savanna between 1990 and 2023. Also, the study showed that degraded areas, stable areas, and improved land represent respectively 21%, 64%, and 15% in the study area from 2001 to 2022. Therefore, we conclude that climate change and demographic pressures have led to the loss of certain natural land cover (tiger bush and savanna), and increased water erosion and the presence of more ephemeral water bodies, subject to excessive evaporation.

Keywords

Land Use, Water Bodies, Dallol Bosso, Niger

1. Introduction

The changes in land use significantly affect hydrological processes and the water regime in the Sahel. The land use changes can significantly impact the water cycle, changing water availability and the water regime as a result of land degradation, urbanization, and agricultural expansion [1] [2]. Understanding these effects is crucial for sustainable land management. This study focuses on the impacts of land use and land cover dynamics on the surface water regime in the Dallol Bosso sub-basin, located in the Tillabéri and Dosso regions of Niger [3]-[6]. The study area is in the Sahelian belt, where the climate is characterized by a short rainy season (June to September) and a long dry season. The average annual rainfall is 561 mm at the Birni N'Gaouré station, in the center of the area, which has favorable land and water potential for the development of agropastoral activities. Therefore, this condition creates competition for access to natural resources and increases the risks of conflicts between users. Several studies have been carried out to show that the effects of climate change and human actions contribute to the continued degradation of soils, vegetation cover, and water bodies, and to the exacerbation of recurring conflicts [7]-[10]. To enable sustainable socio-economic development, taking into account the need for the restoration and protection of ecosystems, it is necessary to understand the inter-relationship between the evolution of land cover and land use in this context of climate change, following the example of recent studies carried out in the Sahel [3] [4]. Hence the general objective of this study, which is to analyze the variations in land cover and land use units and their impacts on the dynamics of water bodies in the study area. To this end, satellite data for the area for the years 1972, 1990, and 2023 were collected and processed, online platforms were used to estimate the state of land degradation, field observation data were analyzed, and thematic maps were established and interpreted. This is a contribution to decision-makers' efforts to preserve the ecosystem better.

2. Study Area

2.1. Geographical and Socio-Economic Situation of the Area

The study area corresponds to the active part of the Dallol Bosso sub-basin, straddling the Dosso and Tillabéri regions in Niger. It lies between longitudes East 3˚48' and 2˚23' and latitudes North 12˚24' - 14˚05' and covers 15,000 km^2 (see **Figure 1**). According to INS's projection [11], the total population of the eight departments (Filingué, Balayara, Ouallam, Kollo, Boboye, Falmay, Loga, Dosso) in the sub-basin is estimated in 2023 at 3,330,635 inhabitants, of whom 50.6% are women.

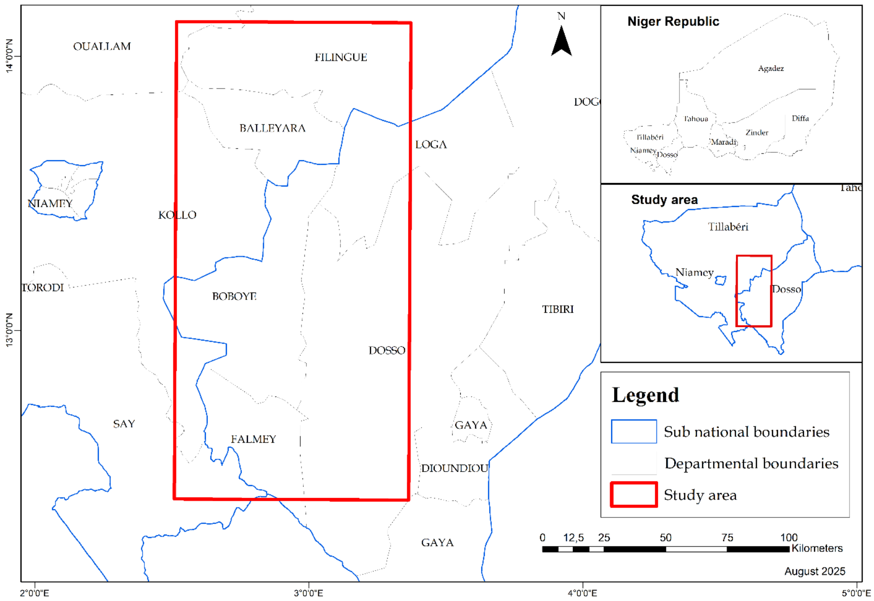

Figure 1. Geographic location of the study area.

Dallol Bosso borders the Niger W Park Biosphere Reserve, which covers 2,200 km^2. It constitutes the eastern buffer zone of the W Park, which contains approximately 80% of Niger's biodiversity, classified since 1996 as a UNESCO World Heritage Biosphere Reserve. The topography of the Dallol Bosso sub-basin is composed of three morphological units: (i) the plateaus that overhang the departments of Baleyara and Filingué in the far north, and the Gaya sector in the south; (ii) the valley zones or paleo-channels of the tributaries of the Niger River between the plateau lines; and finally (iii) the plains or alluvial terraces along the left bank of the Niger River [10]. The three (3) soil types, along the Dallol Bosso Valley from north to south, are:

1) Tropical soils, from the plateaus, form ferruginous and fertile layers when water is available.

2) Valley soils, deposits of sand and clay and/or silty sand.

3) Heavy clay soils of the plains are in the southern part along the river.

The socioeconomic activities in the study area are agriculture, livestock farming, and fishing. Agriculture is rainfed production, with accelerating development of irrigated crops from ephemeral water bodies and shallow alluvial aquifers. Livestock consists of cattle, sheep, goats, camels, and donkeys, herded mainly on barren plateaus and grazing areas on the plains in some valleys.

2.2. Geological and Hydrological Context

The geology of the study area is characterized by the presence of three (3) formations, which are, from bottom to top [10] [12]:

1) Continental Intercalaire/Hamadien (CI/H) formations, consisting of: (i) the Tegama series corresponding to the end of the CI, Albian to Lower Cenomanian in age; (ii) the CH series, medium to coarse sandstones, micaceous and with var-

iegated kaolinitic cement.

2) Continental Terminal Formations (CT), ranging in age from post-Eocene to pre-Quaternary, are a succession of three levels. First, CT1 consists of ferruginous sandstone, ferruginous clays, clays, and ferruginous material; then level CT2 is represented by sands, fine sandstones that are more or less clayey, gray clays, or flaky black muds, characterized by the presence of plant debris [13]. Their thickness increases from west to east to reach more than 80 m at the level of the Bosso dallol [14]. Finally, the level of CT3 is formed at the base by gray clays and outcrops in the form of sandstone plateaus with lateritic shell, covered with tiger bush and cut by erosion. These formations of the CT lie on the crystalline base in the west, where its depth is almost zero (beveling), and can reach more than 130 m towards the east [12].

3) Quaternary deposits and alluvium, consisting of fluvial alluvium that fills the fossil valley of the Dallol and its main tributary, the Azgaret, are present in the northern part. The thickness of the filling is very variable. The thickness varies from a few meters in the valleys of the river and its tributaries to more than 20 m in the Bosso Dallol and a maximum of 15 m in the Azgaret [13].

The hydrogeological context of the study area is characterized by the presence of three (3) main aquifer systems as follows, from bottom to top:

1) Continental Intercalaire/Hamadien aquifer system, containing pressurized water tables, with high depths (300 to 500 m) and fairly high operating flow rates, more than 100 m3/h locally [10] [14]. This is the case for the results of the deep drilling of Dabaga and Birni N Gaouré. These aquifers are present throughout the central part of Dallol Bosso and their exploitation requires deep structures, around 500 m. The waters are quite loaded and, in some sites, they are unfit for consumption.

2) The multi-layered aquifer system of the Continental Terminal (CT1, CT2, CT3), with the first two (2) levels from bottom to top, is under pressure with loaded water. The depths of the water tables vary from 60 m for CT2 and 100 to 150 m for CT1. The third level (CT3) contains an unconfined water table with low-loaded water of good quality for various uses. This is the water table regularly renewed by rainwater infiltration and by exchanges with the alluvial aquifer of Dallol Bosso. Operating flow rates are high, frequently reaching 40 m^3/h.

3) Alluvial aquifers of the Dallol Bosso outcrop and are very thick in the Bonkoukou, Ballayara, and Birni N'Gaouré sectors, where the alluvial deposits are particularly sandy. Large-diameter wells allow specific flow rates that can exceed 10 $m^3/h/m$. In these areas, these aquifers are continuous with the phreatic system of the continental terminal CT3.

The hydrography concerns the presence of the Niger River, the Dallol Bosso, scattered ponds, and intermittent runoff in the fossil valley flowing into the Niger River.

3. Materials and Methods

3.1. Materials

The data used in this study are:

1) Landsat 1, 5, 7, and 8 satellites for the years 1972 (with path/row respectively 207/50, 207/51, 2026/50, and 207/51), 1990, and 2023 (path 206, rows 50 and 51) with a 30 m spatial resolution were provided by USGS glovis.

2) Sentinel 2 satellites with 10 m spatial resolution for the year 2023.

3) Ground observations (water bodies location and regime) were collected from the hydraulic direction in Dosso and Tillaberi.

4) Hydroclimatic data (temperatures, rainfall) from 1972 to 2023 for the stations of Birni N'Gaoure and Filingue were collected from the National Meteorological Service.

5) Water level measurements for the period 2000 to 2022, measured in situ and derived from satellite images.

6) Population of the area of interest from 2012 to 2023.

7) Rainfall at Niamey and Birni N'Gaoure stations from 2012 to 2023.

The data were processed and analyzed using:

1) Google Earth Engine platform.

2) Digital Earth Africa platform.

3) Trends.Earth.

4) ArcGIS 10.8 software.

3.2. Methods

3.2.1. Land Cover and Land Use Classes

In order to compute the land use and land cover, the satellite images (Landsat and Sentinel) were pre-processed [8] [9] [15] [16] with ArcGIS for geo-referencing, mosaicking, and subsetting of the images within the study area. The land use and land cover classes used are those from the Land Use and Land Cover Nomenclature (NOS) of the Ministry in charge of the environment of Niger [17] and were analyzed from optical data during 1972, 1990, and 2023 [15] [16] [18] [19]. Also, high-resolution images were used to validate the series of maps obtained with the Google Earth Engine and Digital Earth Africa platforms. Indeed, the luminance that satellites measure from space is strongly correlated with radiometric data from the ground [3] [4] [15]. Based on its reflectance, the study area was discretized into several surface units [9] [16] [17] [20], corresponding to land use and land cover classes.

The image processing, classification, and analysis followed different steps such as:

1) Color composition with the display of spectral bands in the red, green, and blue channels to highlight the different contrasts.

2) Visual interpretation of the image based on the color composition (Red, Green, Blue) is used to digitize the different land use and land cover classes. This consists of identifying each homogeneous group that represents a specific class.

3) Reduction of misclassifications was addressed by visual interpretation. The visual analysis, referring to local knowledge, considerably improved the land use land cover maps.

3.2.2. Analysis of Land Cover and Land Use Dynamics

The study area is subdivided into 100-meter square grid cells. Within each grid cell, the corresponding land use and land cover class was considered for the years (1972, 1990, and 2023). The post-classification change detection method was conducted using ARCGIS 10. A grid cell by grid cell basis was used to determine the quantity of conversions from one class to another class and their corresponding area [17] over the three periods (1972-1990, 1990-2021, and 1972-2021) [3] [7] [15]. Grids affected by changes will be identified [21].

Periodic changes are calculated using the global change rate formula:

Overall rate of change = (S2 − S1)/S1, with:

S1: the area of the class in the initial year.

S2: the area of the class in the final year.

3.2.3. Analysis of the Land Degradation Evolution

The Trends. Earth tool was used to track Land Degradation Neutrality (LDN) according to the United Nations Convention to Combat Desertification (UNCCD)'s Sustainable Development Goal (SDG) indicator 15.3.1. The land productivity trajectory from 2001 to 2022 was generated to allow a comparison with the local states of the land in the study area.

3.2.4. Analysis of the Evolution of Water Bodies

The surface water frequency, defined as the ratio of wet to clear observations, was derived from the Water Observation from Space (WOfS) [22] algorithm computed with the Digital Earth Africa platform. Water pixels were identified with a minimum frequency threshold of 0.1 (10%) to avoid transient noise and isolated false detections. This algorithm was used to detect the presence of surface water [23]-[25], classify ponds according to the occurrence of water, generate pond curves (surface area, corresponding period), and also the yearly cumulative area and their evolution from 2000 to 2022.

4. Results and Discussion

4.1. Dynamics of Land Cover and Land Use from 1972 to 2023

Land use and land cover were derived from the Landsat 30 m × 30 m spatial resolution during the years 1972, 1990, and 2023. Twelve major land use land cover classes (Degraded tiger bush, Riparian cords, Vegetable farming and lowland crops, Agriculture and fallow land, Kori and ravine, Water body, Bare plateau—Rocky land, Shrubby savanna on glacis, Bare soil—Eroded glacis, Settlement, Eroded slope—Brushwood, and Bare soil—Eroded glacis) were identified. Therefore, the three reference years are considered from the sequence of climatic periods identified after the analysis of the hydro-climatic parameters of the zone (wet period before 1970, dry period from 1970 to 1990, and current period of trend towards a return to normal) [14].

The change detection investigation [21] is applied over approximately fifty-one (51) years (1972 to 2023). Specific units were identified and grouped [26] [27], to correspond to the natural classes for land cover, which are: degraded tiger bush, riparian cords, scrub, bare soil, shrub savanna, flood valley, kori-ravine, ponds, bare plateau, and rocky terrain.

For land use, agriculture and fallow land, settlement, market gardening—lowland crops, were considered [16]. Natural formations [5] [6] [16] [20], and areas related to anthropogenic activities [16] [28] are determined from a visual interpretation of multispectral images in 3 bands for 1972, and in 6 bands for the years 1990 and 2023 [18]. This was done using the combination of the three RGB bands. According to the quality of the Landsat image (cloud coverage), which was primarily used for visual interpretation, Sentinel 2 was used to fill the gap.

4.1.1. Land Cover and Land Use in 1972, 1990, and 2023

The land cover and land use states between 1972 and 2023 are shown in **Figure 2** below [3]-[6].

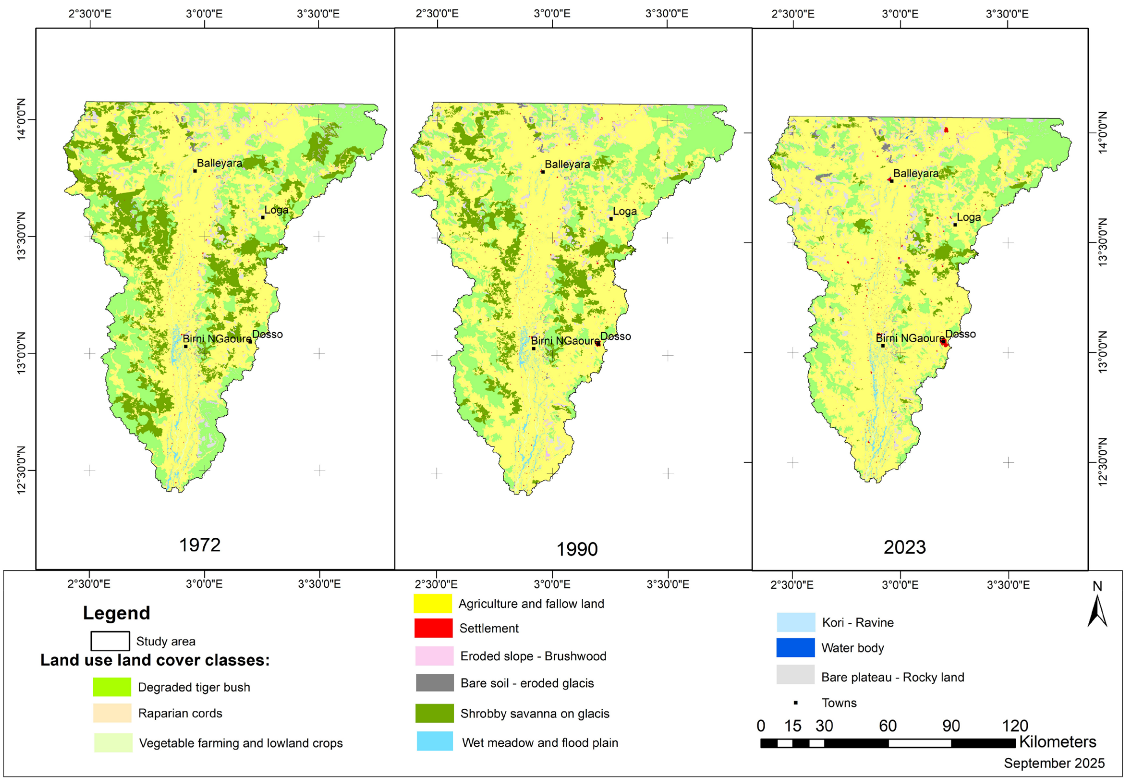

Figure 2. Land use and land cover in 1972, 1990, and 2023.

It is noted that, historically, the land use class has been continuous rainfed agriculture, which is found throughout the entire sub-basin. The second class is tiger bush, which initially covered the entire area and was only found along the lowlands in 2023.

Settlement and bare land or degraded soils are the two smallest classes, found along the riverbed and on the plateaus. The areas and percentages of the different classes as compared to the total area of the sub-basin are shown in **Table 1** below.

Table 1. Land use land cover classes in 1972, 1990, and 2023.

Class:	1972		1990		2023	
Degraded tiger bush	405570	27.04%	348792	23.27%	318140	21.23%
Riparian cords	5189	0.35%	4967	0.33%	5226	0.35%
Vegetable farming and lowland crops	5258	0.35%	5152	0.34%	5193	0.35%
Agriculture and fallow land	765451	51.04%	914642	61.01%	1028614	68.65%
Kori and ravine	700	0.05%	270	0.02%	1201	0.08%
Water body	160	0.01%	457	0.03%	1187	0.08%
Bare plateau—Rocky land	18067	1.20%	21719	1.45%	33176	2.21%
Wet meadow and floodplain	11104	0.74%	11079	0.74%	12470	0.83%
Shrubby savanna on glacy	254256	16.95%	155910	10.40%	49326	3.29%
Bare soil—Eroded glacis	2961	0.20%	4149	0.28%	8500	0.57%
Eroded slope—Brushwood	27745	1.85%	28283	1.89%	28462	1.90%
Settlement	3170	0.21%	3741	0.25%	6820	0.46%

The situation in 1972 was representative of the wet period of the 1960 s [14], and the year 1990 marked a break in the climate dynamics, after the period of droughts between 1972 and 1990 [29]. Natural formations decreased in favor of anthropogenic formations under the combination of human and climate change actions [16] [24]. Thus, with the 2023 land use and land cover maps, the settlement's class increased (doubled) to 0.5% in 2023, 0.25% in 1990, and 0.21% in 1972. However, the situation in 2023 could be the consequence of past droughts and demographic pressures on natural resources, [30], as shown in **Figure 3**.

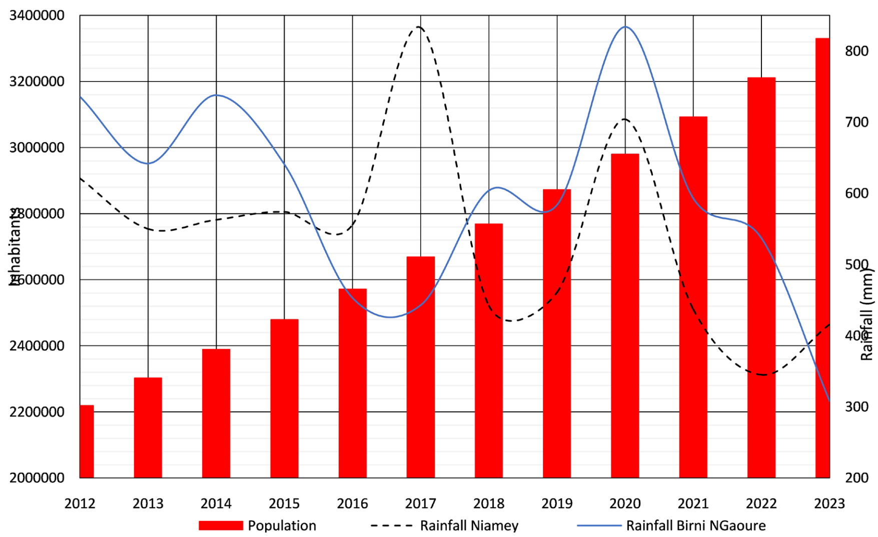

Figure 3. Evolution of the population of the study area and rainfall at Niamey and Birni N'Gaouré.

4.1.2 Evolution of Land Cover and Land Use Classes, 1972-2023

The variation rate of change was computed [4] [6] [20] for each type of class between the different periods and is presented in the following Table 2.

Table 2. Land cover land use change in each class from 1972-1990, 1990-2023, and 1972-2023.

Land use land cover classes	Changes in land use land cover classes					
	1972-1990		1990-2023		1972-2023	
	Ha	%	ha	%	ha	%
Degraded tiger bush	−56,778	−14%	−30,652	−9%	−87,430	−22%
Riparian cords	−222	−4%	259	5%	37	1%
Vegetable farming and lowland crops	−106	−2%	41	1%	−65	−1%
Agriculture and fallow land	149 191	19%	113,972	12%	263,163	34%
Kori and ravine	−430	−61%	931	345%	501	72%
Water body	297	186%	730	160%	1,027	642%
Bare plateau—Rocky land	3,652	20%	1,1457	53%	15,109	84%
Wet meadow and floodplain	−25	0%	1391	13%	1,366	12%
Shrubby savanna on glacy	−98 346	−39%	−106,584	−68%	−204,930	−81%
Bare soil—Eroded glacis	1 188	40%	4,351	105%	5,539	187%
Eroded slope—Brushwood	538	2%	179	1%	717	3%
Settlement	571	18%	3 079	82%	3 650	115%

Between 1972 and 1990, there was a decrease in the following classes: degraded tiger bush, shrub savannas on glacis, and koris. These class-level decreases, despite the onset of the wet season, could be explained by the persistence of the negative impacts of the drought during the years 1972-1973 and 1983-1984, [31]. The classes that increased during this period were bare soils (40.1%), bare plateaus (20.2%), agriculture and fallow land (19.5%), and settlement (18%). Thus, over the past 34 years (between 1990 and 2023), it can be noted that the tiger bush and shrub savanna have declined considerably, by 1,332 hectares per year for the tiger bush and 4,634 hectares per year for the shrub savanna.

Settlement increased by 80% and agricultural and fallow areas by 12%. This period is characterized by an expansion of the areas of classes linked to water availability (ponds, koris, agriculture). Degraded lands and glacis increased due to demographic pressure. The land use and land cover change dynamics for the years 1972, 1990, and 2023 are represented in Figure 4(a)-(c).

Figure 4(a) highlights a uniformity observed for the classes' riparian cords, vegetable farming and lowland crops, and eroded slope—Brushwood from 1972 to 2023, whereas an increase was observed for the bare plateau and rocky land class.

Figure 4(b) shows that from 1972 to 2023, the classes of water body, settlement, and bare soil-eroded glacis increased considerably. The maximum is observed in 2023.

Figure 4(c) illustrates a decrease in the shrubby savanna on glacy and degraded tiger bush observed from 1972 to 2023. The minimum values were reached in 2023 and the maximum in 1972. Over the same period, agriculture increased from its lowest value in 1972 to the highest in 2023.

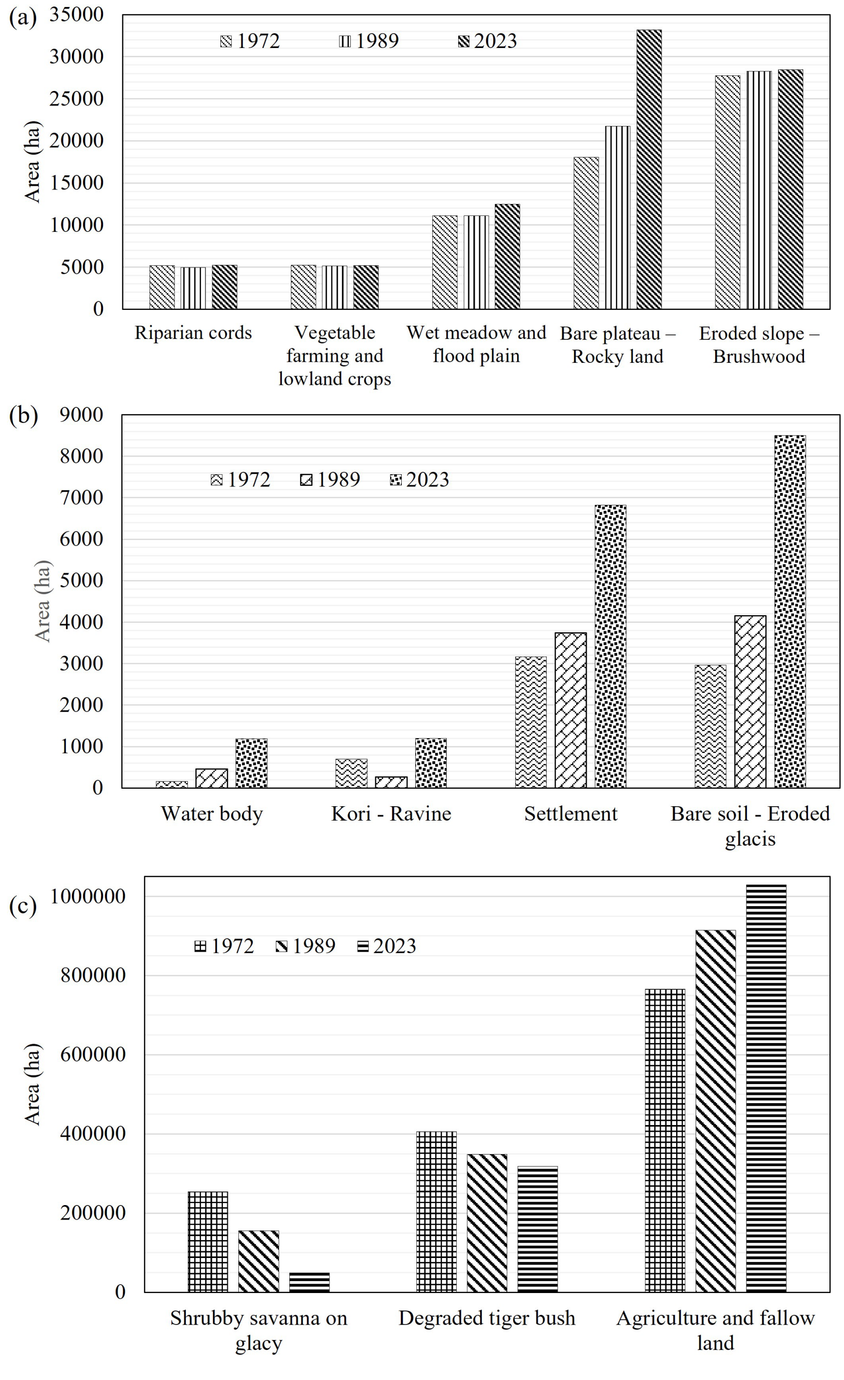

Figure 4. (a) Land use and land cover change dynamics of riparian cords, vegetable farming, wet meadow, bare soil, and eroded slope; (b) Land use land cover change dynamics of water bodies, kori, settlements, and bare soil-eroded glacis; Land use land cover change dynamics of shrubby savanna on glacy, degraded tiger bush, and agriculture and fallow land.

Over the period from 1972 to 2023 (51 years), the same trends were confirmed due to the increase in demographic pressure and the persistence of the impacts of climate change. Indeed, in 2023, crops and fallow land occupied 68.7% of the area, with degraded tiger bush occupying 21.7% and shrub savanna on glacis at 3.3%, compared to 10.4% in 1990. Floodplain valleys, koris, and ponds increased in area at the expense of vegetation.

This dynamic could be linked to the rainfall regime in the area [23] [24], which is characterized by:

1) An initial wet period before 1972, with normal rainfall favoring the development of vegetation and runoff and gully erosion. Population density was low and agricultural land was undeveloped.

2) A dry period from 1972 to 1990, with low rainfall, led to deforestation and the particular development of runoff and gully erosion. Water concentrated in the lowlands disappeared a few days after the rainfall, due to evaporative pressure.

3) A period of return to normal rainfall after 1990, with surplus years and natural regeneration, resulted in reduced runoff.

This trend has exacerbated the risks of conflict for access to land, particularly in areas where farmers and herders are concentrated (Boboye Department) [32].

4.1.3. Conversions of Classes between 1972, 1990, and 2023

Between 1972 and 2023, the dynamics of land use and land cover show the increase in cultivated area. Indeed, 90,000 ha of tiger bush and 193,000 ha of savanna were converted into agricultural land. Also, between 1972 and 1990, 67,000 ha of tiger bush and 97,000 ha of shrub savanna were converted into agricultural land, and between 1990 and 2023, 33,763 ha of tiger bush and 100,934 ha of shrub savanna on glacis were converted into agricultural land. This confirms the impacts of demographic pressure and climate change [16].

4.2. Dynamics of Degraded Lands

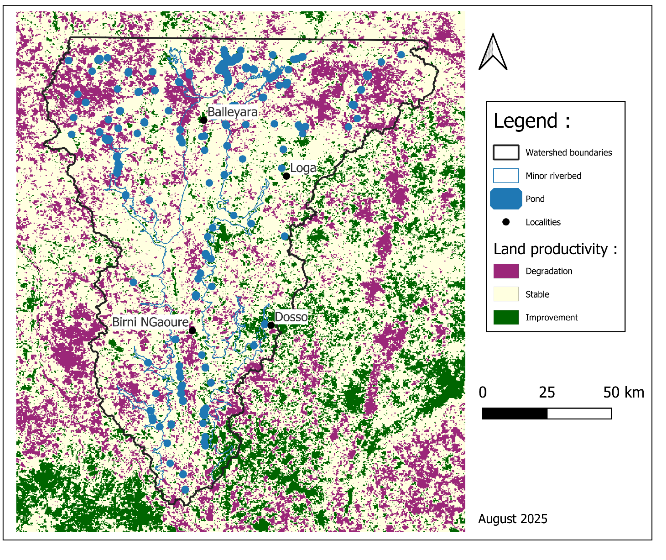

Figure 5. Land productivity trajectory from 2001 to 2022 in the study area (SDG 15.3.1).

The investigation of the land's degradation was computed using Trends. Earth to determine the land productivity trajectory in the study area [5] [6] [20]. Three situations are represented with land in continuous degradation, stabilized land, and restored or improved land (SDG Indicator 15.3.1) [33], as illustrated in **Figure 5**.

It is noted that degraded areas represent 21%, stable areas represent 64%, and restored or improved land represents 15% in the study area from 2001 to 2022. Degraded land is mainly in the northern part of the study area, where the tiger bush and vegetation classes have been converted to agricultural land or crusted bare land.

4.3. Dynamics of Water Bodies in the Study Area

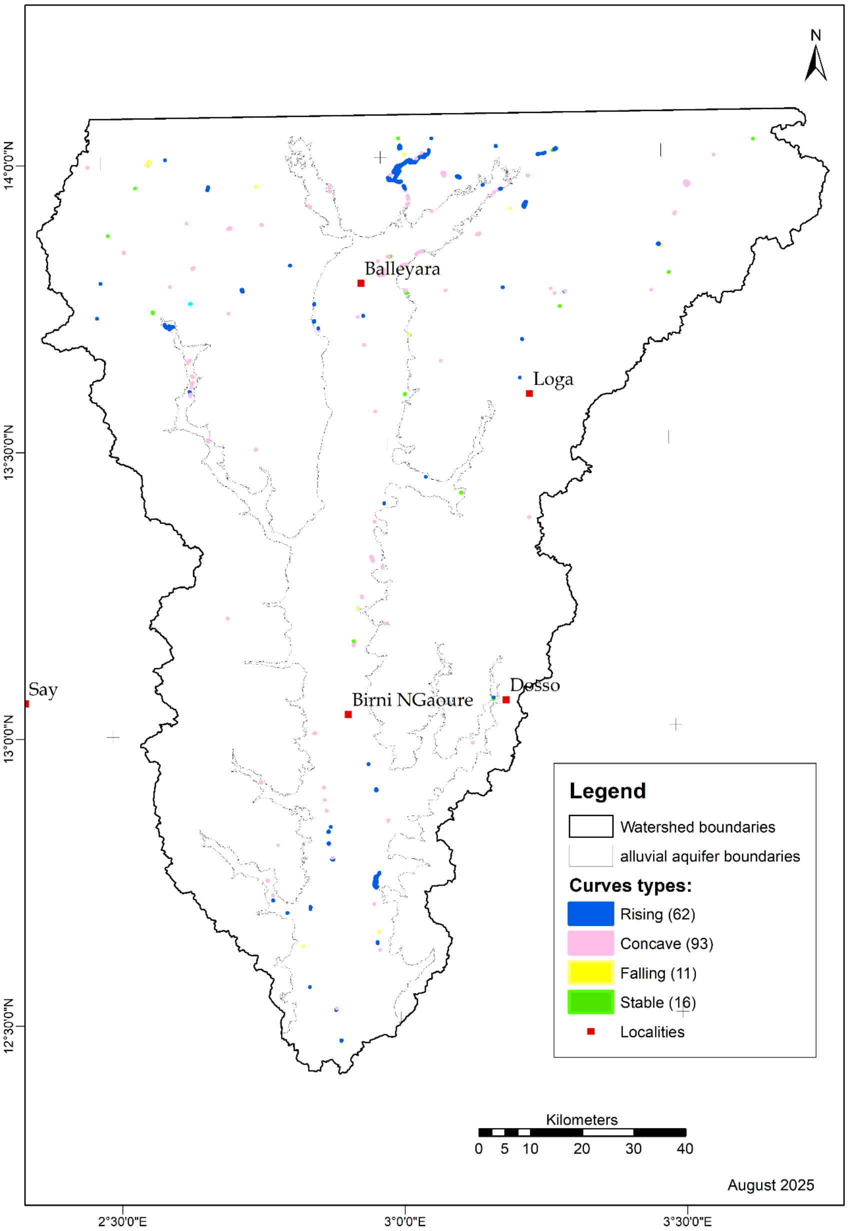

Figure 6. Water body's curve type distribution.

The values of the Modified Normalized Difference Water Indices (MNWI) were derived [19] [22] in order to analyze the spatial distribution of the water bodies in the study area. Thus, for the month of August 2023, the indices show the presence of one hundred and eighty-two (182) surface water bodies in the study area, among which 65.38% (119) were concentrated in the northern part, 16.48% (30) in the center, and 18.13% (37) in the south, as illustrated in **Figure 6**, locating the ponds. The spatial distribution of water bodies is correlated with the dynamics of land degradation and with changes in land cover and land use, [3] [5] [23] [24].

Indeed, runoff and ponds (ephemeral and semi-permanent) are concentrated in areas of land crusting and agricultural development. Shrubby savannas are converted into agricultural land or bare slopes, promoting runoff and the formation of water bodies in lowlands [6] [20].

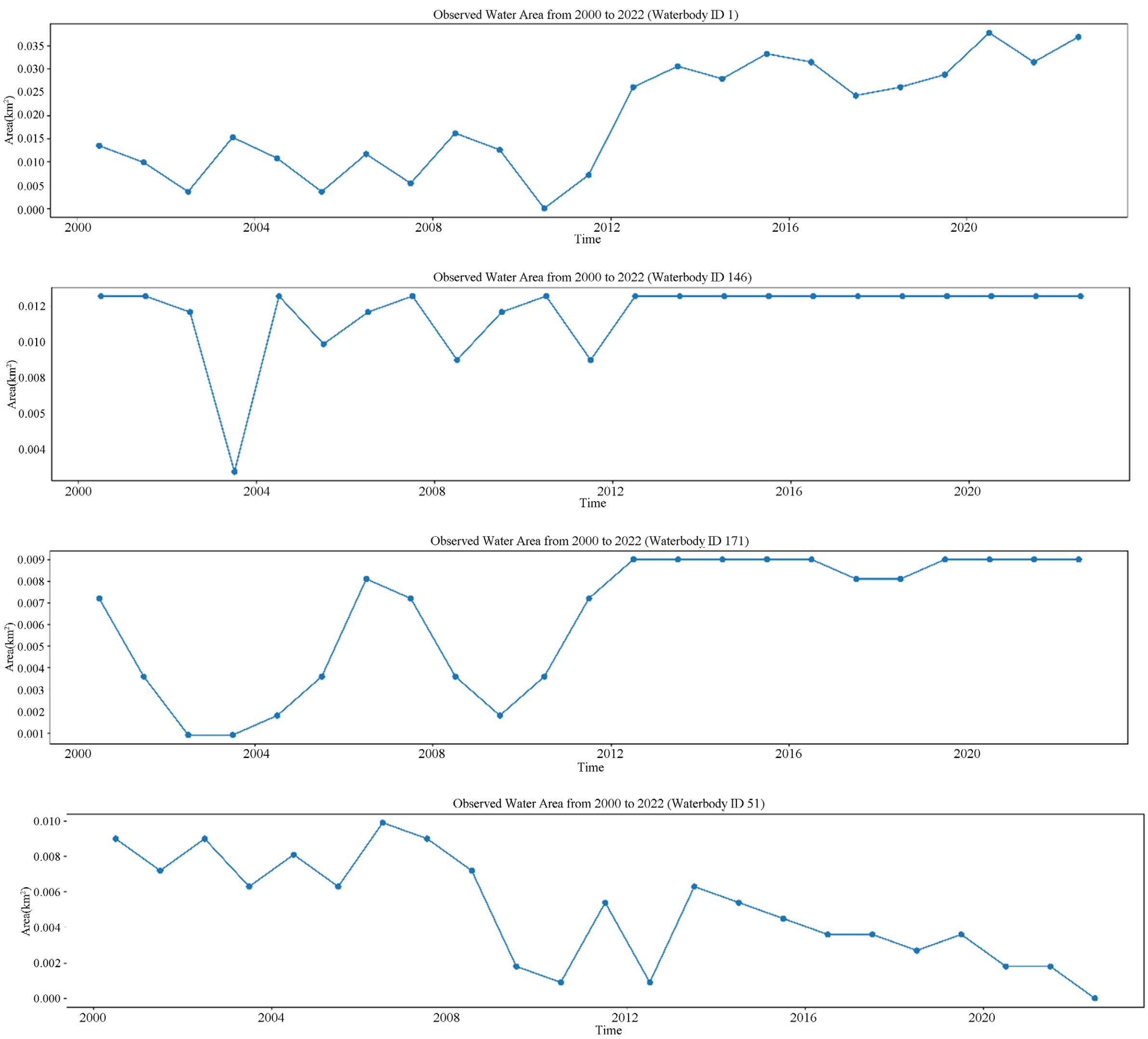

Figure 7. Waterbody Curves from 2000 to 2022: (a) ascending, (b) concave, (c) stable, and (d) descending.

Based on the values of the occurrence and sections of the water bodies captured by the satellite on the same dates for successive years from 1972 to 2023, the ponds are classified into four (4) types (**Figure 7**) [19] [23]:

1) Ascending curves represent water bodies with increased cross-sections or volumes each year throughout the entire analysis period (1972-2023). These are ponds that did not experience a decrease in surface area during this period.

2) Concave curves represent water bodies that lost surface area or even disappeared during the drought period and began to recover their capacity with the return of rainfall.

3) Descending curves represent ponds that have maintained a constant rate of decrease in surface area since the beginning of the observation period.

4) Stable curves characterize monotonous water bodies, where capacity remains the same.

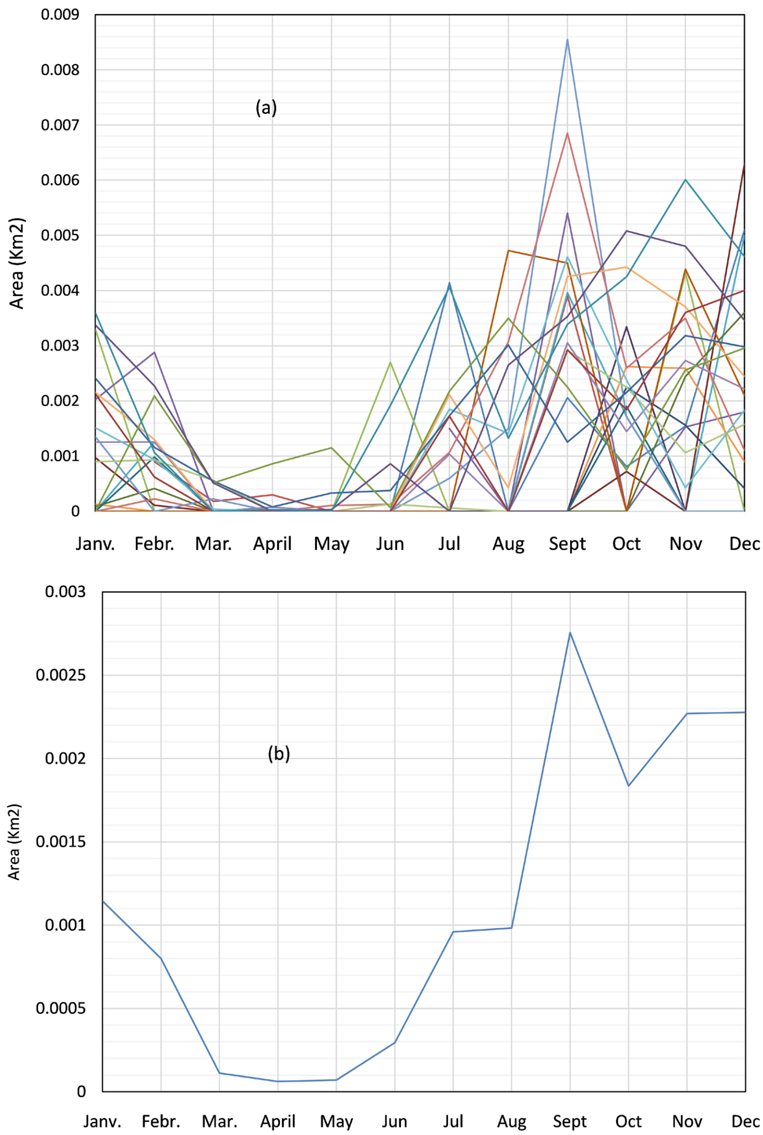

Figure 8. Permanent ponds graph (a) yearly water surface area (b) mean of water surface area from 2000 to 2022.

Figure 8(a) showed the positive value of water surfaces, which indicated the presence of water bodies during all the years, and Figure 8(b) confirmed the same result with minimum values from April to June and maximum values from August to November each year.

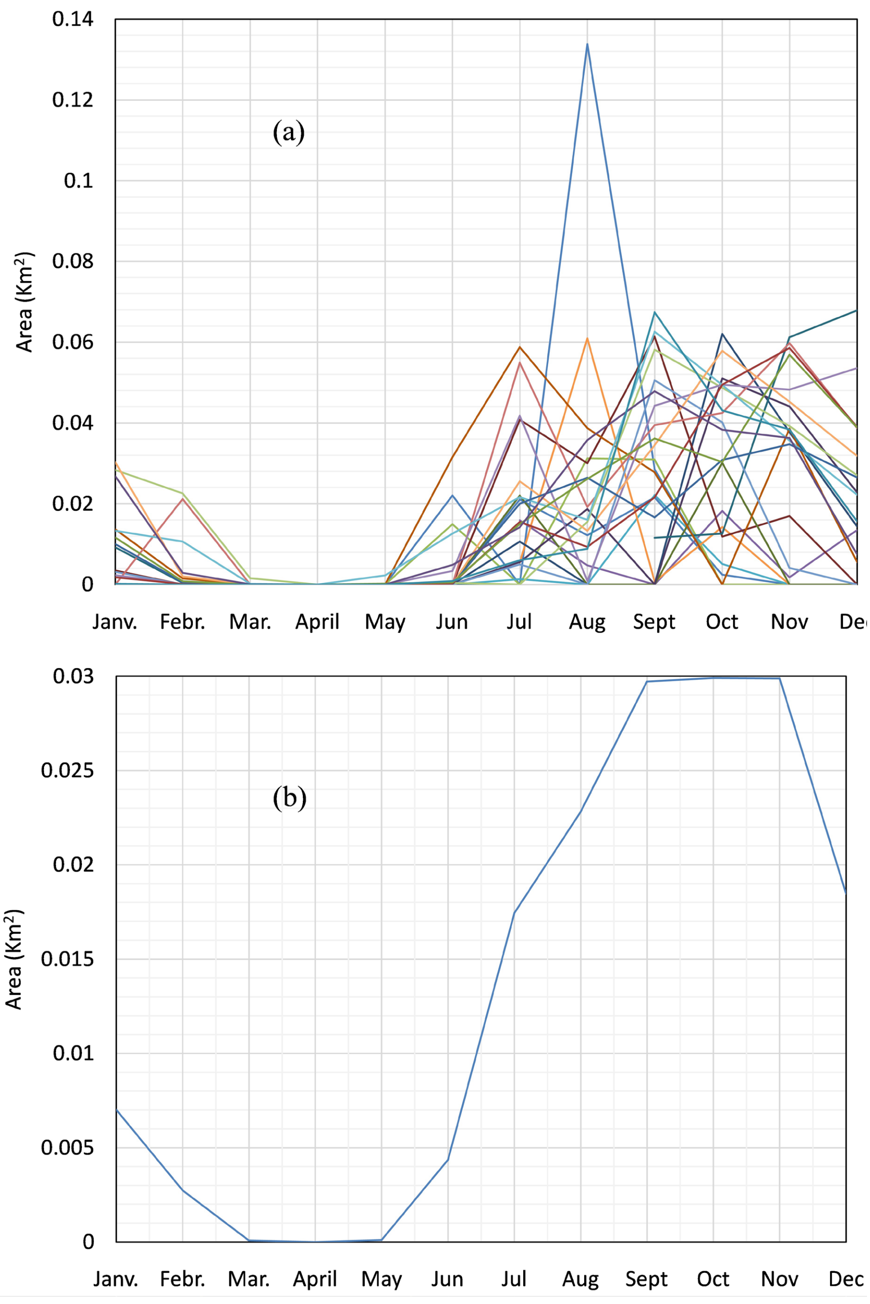

Figure 9. Semi-permanent ponds graph (a) yearly water surface area (b) mean of water surface area from 2000 to 2022.

Figure 9(a) showed the absence of a water body during a short period of the year, particularly in April and May, and in March according to some years. Figure 9(b) confirmed the same result with an absence of water from March to May, announcing the beginning of the rainy season.

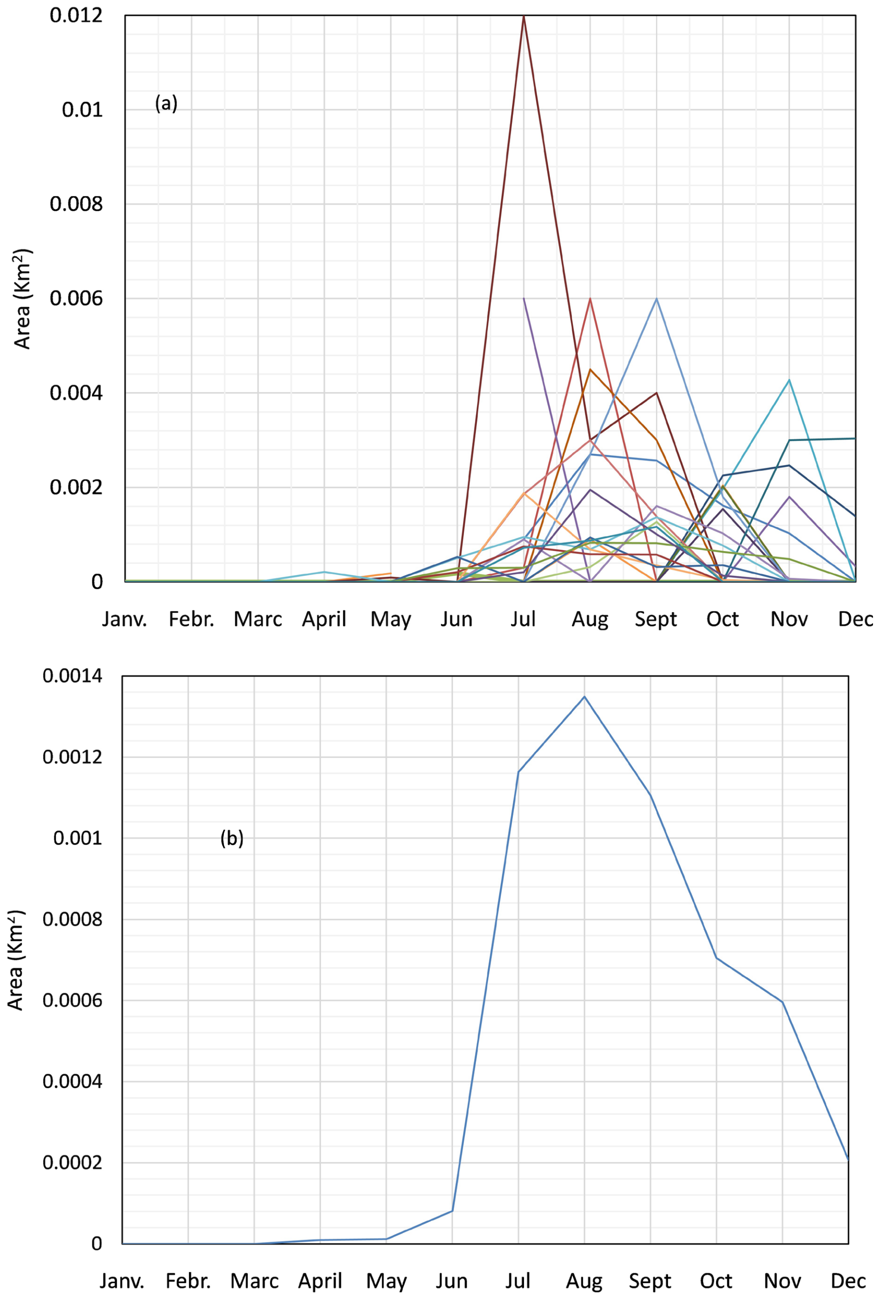

Figure 10. Ephemeral ponds graph (a) yearly water surface area (b) mean water surface area from 2000 to 2022.

Figure 10(a) shows the absence of a water body during the period from January to March. **Figure 10(b)** confirms the same result, with the absence of water from January to May.

Among the 182 water bodies or ponds:

1) Sixty-two ponds are ascending, indicating that the regime of these ponds is increasing in terms of capacity and surface area. Forty-three (43) of these ponds

are concentrated in the north and nineteen (19) in the south.

2) Sixteen ponds are stable in shape, corresponding to identical surface areas, not varying over time, over the period. Thirteen (13) ponds in this group are in the northern part of the sub-basin and three (3) in the south in the low-flow channel.

3) Ninety-three ponds are concave, indicating shrinking regimes of these ponds during the first part of the period and a return with a recovery of capacity thereafter depending on climatic conditions and.

4) 11 ponds are linear and descending, indicating, over the entire monitoring period, a decline in surface area and water retention capacity.

Following this analysis, permanent ponds with water present throughout the year, semi-permanent ponds with water present from the end of the rainy season to March or April, and ephemeral ponds with water present until December were identified. This situation is illustrated in **Figures 8-10**.

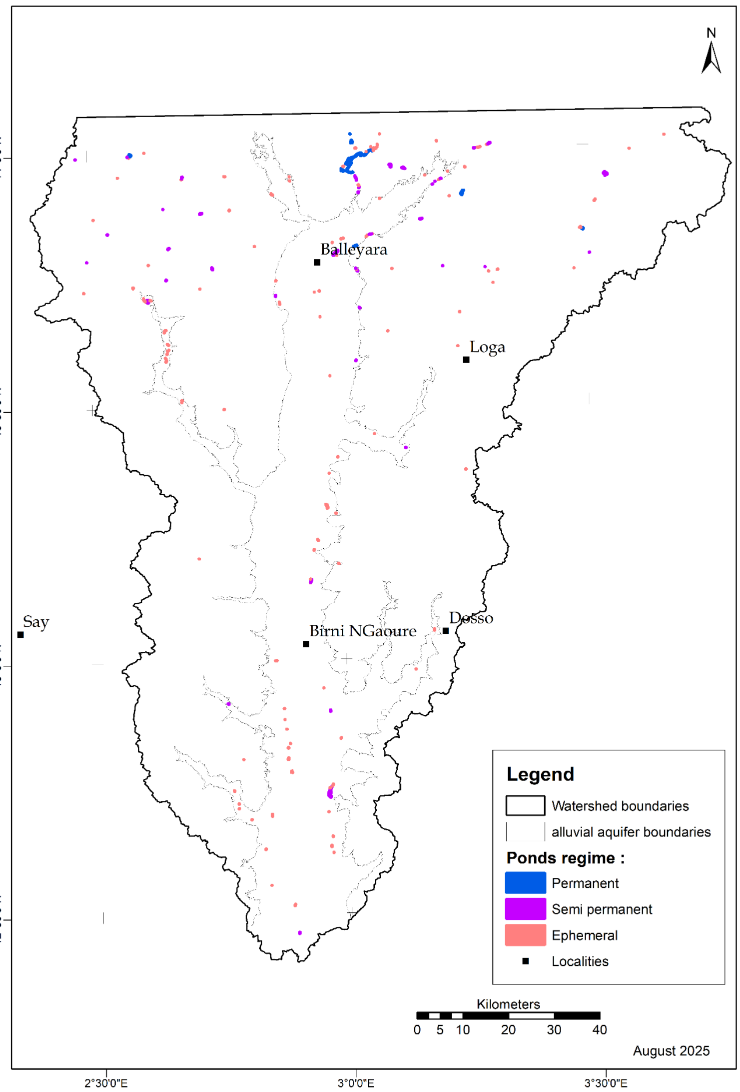

Figure 11. Water bodies' yearly regime in the study area.

A total of eight (8) permanent ponds, forty-one (41) semi-permanent ponds, and one hundred and thirty-three (133) ephemeral ponds are identified, **Figure 11**. All the permanent ponds are located in the northern part of the study area beyond the latitude of Balleyara. This presence enables the possibility of exchange between the pond and the aquifer. Among the forty-one (41) semi-permanent ponds, six (6) are located in the south and thirty-five (35) in the north. The ephemeral ponds are scattered throughout the study area.

The annual patterns of water bodies depend on the location of the pond (land degradation context), the start date of the rainy season, and the quantity of rainfall (surplus, normal, or deficit years). Indeed, we note that:

1) The response time for the resumption of pond filling depends on the geographical position and morphology of the area. Depressions at the foot of the plateaus receive the first runoff. Ponds located in the plains have longer response times.

2) The appearance of the graphs indicates the pond regimes (ephemeral to permanent). The presence of a permanent pond with direct water infiltration could help to locate preferential areas for the recharge of alluvial aquifers.

3) The presence of degraded lands to the north of the study area favors the appearance of water bodies (strings of ponds) [23] [24] [34].

5. Conclusion

Land use and land cover are the consequence of a complex set of parameters that range from natural processes to anthropogenic intervention. This study focuses on the change in land cover and land use units and their impacts on the dynamics of water bodies in the study area from 1972 to 2023. Also, the relationship between land cover and land use dynamics and the evolution of water bodies was investigated. In the study area, climate change and demographic pressures have led to the loss of certain natural land cover (tiger bush and savanna), and improved the surface runoff and the presence of ephemeral water bodies, subject to excessive evaporation. Also, it is noted that agricultural production has affected soil quality (soil crusting and gullying). This has a direct impact on the local population and the ecosystem. This study contributed to both ecologists and managers working at the national and local scales. It benefits ecologists through an understanding of patterns and dynamics which affect landscape processes and enables decision-makers to put in place mechanisms for effective water resource management in the study area. For a better understanding of the dynamics of land use and land cover and their impact on the regime of water bodies, it is necessary to maintain and enhance the continuous quantitative and qualitative monitoring of groundwater and surface water resources in the area with the aim of developing a hydrological model.

Acknowledgements

The co-authors of this article would like to thank:

1) Niger's Ministry of Environment, Hydraulics, and Sanitation.

2) Rural Hydraulics Program to support Water and Sanitation Sectors (PHRASEA), funded by Swiss Cooperation in Niger.

3) The IGO HELVETAS' representatives in Niger, implementing agency for PHRASEA.

These organizations funded the data collection and processing, making this article possible.

Conflicts of Interest

All authors declare no conflict of interest in this publication.

References

[1] Namugize, J.N., Jewitt, G. and Graham, M. (2018) Effects of Land Use and Land Cover Changes on Water Quality in the Umngeni River Catchment, South Africa. *Physics and Chemistry of the Earth*, *Parts A*/*B*/*C*, **105**, 247-264. https://doi.org/10.1016/j.pce.2018.03.013

[2] Mansour, M. (2015) Assessing Soil Erosion Risk in the Tillabery Landscape, Niger. *African Journal of Environmental Science and Technology*, **9**, 176-191. https://doi.org/10.5897/ajest2014.1731

[3] Mbala, L.K., Nitu, G.P.M, Djamba, A.M. and Idrissa, I.E. (2024) Analyse spatio-temporelle de l'occupation des sols dans le secteur de Mawanga. *International Journal of Innovation and Applied Studies*, **42**, 243-251.

[4] Mbaiyetom, H., Tientcheu, M.L.A., Ngankam, M.T., Taffo, J.B.W. and Tanougong, A.D. (2020) Dynamique spatio-temporelle de l'occupation du sol et du couvert végétal des parcs arborés du Département de la Nya, Sud du Tchad. *International Journal of Innovation and Applied Studies*, **31**, 370-379.

[5] Kouamé, K.A., Koudou, A., Kouamé, K.F., Kouassi, A.M., Oularé, S. and Adon, G.C.R. (2015) Evolution de l'occupation du sol et rythme saisonnier de la végétation du bassin versant du Bandama en Côte d'Ivoire. *Revue Ivoirienne des Sciences et Technologie*, **26**, 173-193.

[6] Tankoano, B., Hien, M., Dibi, N.H., Sanon, Z., Yameogo, J.T. and Somda, I. (2015) Dynamique spatio-temporelle des savanes boisées de la forêt classée de Tiogo au Burkina Faso. *International Journal of Biological and Chemical Sciences*, **9**, 1983-2000. https://doi.org/10.4314/ijbcs.v9i4.23

[7] Aka, K.P., Koffi, Y.B., Kamagate, A., Ahoussi, K.E. and Kouassi, A.M., (2024) Evolution de l'occupation du sol dans les bassins versants fortement urbanisés et leurs impacts sur les ruissellements de surface: Cas de Bonoumin et du Gourou (Abidjan, Côte d'Ivoire, Afrique de l'Ouest. *International Journal of Innovation and Applied Studies*, **41**, 729-744.

[8] Bou Kheir, R., Girard, M.C., Shaban, A., Khawlie, M., Fouar, G. and Darwirch, T. (2001) Apport de la télédétection pour la modélisation de l'érosion hydrique des sols dans la région côtière du Liban. *Télédétection*, **2**, 79-90.

[9] Stéphane, K.A., Roland, A. and Jalal, E.M. (2020) Utilisation d'une image satellite LANDSAT 8 pour la cartographie de l'occupation des sols dans la ville de Bondoukou et ses environs en Côte d'Ivoire. *International Journal of Innovation and Applied Studies*, **30**, 153-161.

[10] Saley, A.K.H., Sandao, I., Garba, I.S., Ambarka, B.M. and Idrissa, M. (2025) Dynamics

of the Alluvial Aquifer in the Northern Part of the Dallol Bosso and Assessment of Water Potential for Small-Scale Irrigation: Departments of Balleyara and Filingué. *International Journal of Biological and Chemical Sciences*, **18**, 1884-1905. https://doi.org/10.4314/ijbcs.v18i5.21

[11] Institut National de la Statistique du Niger (INS) (2017) Annuaire Statistique 2023-2027 edition 2018.

[12] Gregeirt, J. (1978) Atlas des eaux souterraines de la République du Niger. Etat des connaissances [Rapport BRGM, 79 AGE001].

[13] Tirat, M. (1964) Contribution à l'étude hydrogéologique du Continental Terminal. Rapport BRGM, NIA.64. A1, 77.

[14] Favreau, G. (2000) Caractérisation et modélisation d'une nappe phréatique en hausse au Sahel. Master's Thesis, Université Paris-Sud.

[15] Patrick, Y.A., Ernest, A.K. and Aristide, Y.K.S. (2023) Cartographie par télédétection des changements de l'occupation du sol à partir des images Landsat dans une zone d'orpaillage, département de Dimbokro (Centre-Est, Côte d'Ivoire. *International Journal of Innovation and Applied Studies*, **40**, 247-257.

[16] Kangah, A. (2006) Utilisation de la télédétection et d'un système d'information géographique (SIG) pour l'étude des pressions anthropiques sur les paysages géomorphologiques des savanes sub-soudanaises: Exemple du degré carré de Katiola (centre-Nord ivoirien). Master's Thesis, Université de Cocody-Abidjan.

[17] MHE Niger (2001) Nomenclature pour la construction de bases de données sur l'occupation des sols au Niger au Sud du 16ème parallèle. NOS, Direction de l'Environnement, 69.

[18] Kouadio Bi, V., Ouattara, B., Tankam, A., Fotsing, N., Djagoua, J., Kouamé, E., Affian, F., Borda, K. and Tonye, E. (2016) Apport des champs de Markov à la classification des images multispectrales landsat TM, ETM+ et OLI du département de Sinfra (Centre-Ouest de la Côte d'Ivoire) [Contribution of Markov Random Field (MRF) to Landsat Multispectral TM, ETM+ and OLI Images Classification, of the Department of Sinfra (West-Center of Côte d'Ivoire)]. *International Journal of Innovation and Applied Studies*, **17**, 407-423.

[19] Bako, M. (2020) Application de l'imagerie satelliatire à l'invenatire et au suivi des eaux souterraines: Cas du bassin du Goulbi N'Maradi. Ph.D. Thesis, Université Abdou Moumoni.

[20] Girard, M.C. (1995) Apport de l'interprétation visuelle des images satellitaires pour l'analyse spatiale des sols. Étude et Gestion des Sols. https://www.afes.fr/wp-content/uploads/2023/04/EGS_2_1_GIRARD

[21] Hamidou, A., Boubé, M., Mahamane, A., Mahamane, S. and Abassa, I. (2012) Caractérisation de la dynamique spatio-temporelle de l'occupation des terres dans le complexe des forêts de classées de Dan kada Dodo-Dan Gado (région de Maradi, Niger). *Journal des Sciences de l'Environnement*, **1**, 16-26.

[22] Halabisky, M., Mubea, K., Mar, F., Yuan, F., Burton, C., Birchall, E., Moghaddam, N.F., Adimou, G., Mamane, B., Ongo, D., Boamah, E., Chong, E.F., Gandhi, N., Leith, A., Hall, L. and Lewis, A. (2022) Water Observations from Space: Accurate Maps of Surface Water through Time for the Continent of Africa. https://doi.org/10.1002/essoar.10510203.1

[23] Kouamé, A.K., Adon, C.G., Kouassi, M.A., Koudou, A. and Kouamé, F.K. (2019) Impact de la répartition spatiale de la pluviométrie et de l'occupation du sol sur la recharge des aquifères du bassin versant du Bandama en Côte d'Ivoire. *International Journal of Innovation and Applied Studies*, **27**, 1024-1036.

[24] Kouassi, A.M. (2007) Caractérisation d'une modification éventuelle de la relation pluie-débit et ses impacts sur les ressources en eau en Afrique de l'Ouest: Cas du bassin versant du N'zi (Bandama) en Côte d'Ivoire. Master's Thesis, Université Félix Houphouët Boigny de Cocody.

[25] Fossou, N.M.R. (2015) Variabilité de la pluviométrie et son incidence sur les ressources en eau, les écosystèmes environnementaux et modélisation hydrologique dans les départements de Bocanda et de Dimbokro (Centre-Est de la Côte d'Ivoire en Afrique de l'ouest). Master's Thesis, Université Félix Houphouët Boigny de Cocody.

[26] Mensah, F., Mushtaq, F., Bartel, P., Abramowitz, J., Cherrington, E., Mahamane, M., *et al.* (2024) Land Cover Mapping in West Africa: A Collaborative Process. *Land*, **13**, Article 1712. https://doi.org/10.3390/land13101712

[27] Mahamane, M., Di Gregorio, A., Henry, M., Mensah, F., Bartel, P., Mamane, B., Cherrington, E., Muench, R., Abramowitz, J., Olofsson, P., Singh, A., Judge, J., Brink, A., Dieye, A., Hackman, K., Dawson, M. and Neya, O. (2021) West Africa Land Use/Land Cover Harmonisation Task Force for ECOWAS. AGU Fall Meeting Abstracts, GC25B-0664.

[28] Abdou Mahaman, R., Nazoumou, Y., Favreau, G. and Issoufou Ousmane, B. (2022) Dynamique d'occupation et d'utilisation des sols et la hausse de la nappe dans la basse vallée du Dallol Maouri. *European Scientific Journal*, *ESJ*, **18**, 162-179. https://doi.org/10.19044/esj.2022.v18n14p162

[29] Gansaonré, R.N. (2018) Dynamique du couvert végétal et implications socio-environnementales à la périphérie du parc W/Burkina Faso. *VertigO*, **18**, 20. https://doi.org/10.4000/vertigo.20249

[30] Guengant, J.P., Banoin, M., Quesnel, A., Gendreau, F. and Lututala, M. (2003) Dynamique des populations, disponibilités en terres et adaptation des régimes fonciers: Le cas du Niger. https://www.academia.edu/download/119396786/39844345

[31] Ozer, P. (2004) Bois de feu et déboisement au Sahel: Mise au point. *Revue Sécheresse*, **15**, 243-251. https://orbi.uliege.be/handle/2268/15737

[32] Oumarou, A. (2012) Dynamique du Pulaaku dans les sociétés peules du Dallol Bosso (Niger). 1-290. https://www.torrossa.com/en/resources/an/4946512

[33] Mahamane, M., Mamane, B., Siradji, A.A., Saidou, A.R., Toukal, B., Oulame, S.A., Nteziryayo, R.L. and Abdou, M.R. (2025) Suivi des sites de restauration des terres dans les communes de Dan Kassari, de Matankari, de Dogon Kirya, de Allela et de Birnin Konni ; Niger. *African Scientific Journal*, **3**, 349-375. https://doi.org/10.5281/zenodo.16738967

[34] Abdou, O.M., Habou, R., Soumana, I. and Guimbo, I.D. (2024) Etude de la dynamique de l'occupation du sol dans la commune de Tondikiwindi dans l'ouest-nigérien. *African and Mediterranean Agricultural Journal*, **145**, 49-59. https://doi.org/10.34874/IMIST.PRSM/afrimed-i145.50430